LBNL-40953
Preprint

ERNEST ORLANDO LAWRENCE BERKELEY NATIONAL LABORATORY

Spectral Response of Multi-Element Silicon X-Ray Detectors

C. Rossington Tull, B.A. Ludewigt, and D. Lewak

Engineering Division

November 1997

Invited paper submitted to
IEEE Transactions on Nuclear Science

REFERENCE COPY
Does Not
Circulate
Bldg. 50 Library - Ref.
Lawrence Berkeley National Laboratory
LBNL-40953
Copy 1

DISCLAIMER

This document was prepared as an account of work sponsored by the United States Government. While this document is believed to contain correct information, neither the United States Government nor any agency thereof, nor the Regents of the University of California, nor any of their employees, makes any warranty, express or implied, or assumes any legal responsibility for the accuracy, completeness, or usefulness of any information, apparatus, product, or process disclosed, or represents that its use would not infringe privately owned rights. Reference herein to any specific commercial product, process, or service by its trade name, trademark, manufacturer, or otherwise, does not necessarily constitute or imply its endorsement, recommendation, or favoring by the United States Government or any agency thereof, or the Regents of the University of California. The views and opinions of authors expressed herein do not necessarily state or reflect those of the United States Government or any agency thereof or the Regents of the University of California.

LBNL-40953
UC-406

Spectral Response of Multi-Element Silicon X-Ray Detectors

C. Rossington Tull
B.A. Ludewigt
D. Lewak

Engineering Division
Ernest Orlando Lawrence Berkeley National Laboratory
University of California
Berkeley, CA 94720

November 1997

This work was supported by the Director, Office of Energy Research, Office of Biological and Environmental Research, of the U.S. Department of Energy under Contract No. DE-AC03-76SF00098.

Spectral Response of Multi-Element Silicon X-Ray Detectors

C. Rossington Tull,[1] B.A. Ludewigt,[1] and D. Lewak[2]
[1] Lawrence Berkeley National Laboratory,
1 Cyclotron Road, Berkeley CA, 94720
[2] Microprose, Inc., Alameda, CA

Abstract

An x-ray spectrometer combining multi-element silicon detectors and multi-channel integrated circuit pulse-processing electronics is being developed for low noise, high count rate synchrotron x-ray fluorescence applications. This paper reports on the issues surrounding the use of highly segmented silicon detectors for x-ray spectroscopy. Several different detector geometries were modeled using commercially available device simulation software, and selected geometries were fabricated using planar processing techniques on high resistivity silicon. The detectors were characterized using a 5 μm diameter 8.5 keV x-ray beam, and ^{55}Fe and ^{109}Cd radioisotope sources. Spectral background, anomalous peaks, peak-to-background and charge sharing between adjacent detector elements were studied. The measured x-ray spectral responses are interpreted with respect to the device simulations. These measurements bring to light the effects of detector design, detector processing techniques and detector materials properties on the spectral response of the detector. [1]

I. INTRODUCTION

Multi-element silicon detectors, fabricated from high resistivity silicon using planar processing techniques, have been under development for high energy physics particle detectors for a number of years. We have adapted one of the high energy physics one-dimensional strip detector designs for use in x-ray fluorescence applications. Our primary goal has been to develop multi-element detectors for high count rate, low noise synchrotron x-ray fluorescence (XRF) and x-ray absorption spectroscopy (XAS) [1] applications. Typical XRF and XAS experiments require detectors with very good energy resolution (on the order of 150-200 eV FWHM at 6 keV) and high count rate capability (on the order of several MHz per cm^2, depending on the experiment). Single element, and multi-element lithium-drifted silicon (Si(Li)) and high purity germanium (HPGe) detectors are often used by synchrotron XRF and XAS experimenters, as these types of detectors provide excellent energy resolution. The cost of these detector systems is quite high (≈$10,000/channel) and the physical configuration of such detectors is limited due to the size of the detectors and electronics. In addition, the Si(Li) and HPGe detectors require cryogenic cooling, which adds to the cost and mechanical limitations in the design of such detectors. To address the need for a more flexible detector design, and to offer a more cost-effective approach to multi-element semiconductor detector design, we are developing multi-element silicon detectors fabricated on high resistivity silicon substrates, using planar processing and photolithographic techniques to subdivide the single crystal substrate into many detector elements. These detectors are designed to detect x-rays in the 0.5 - 25 keV range, with an energy resolution of <200 eV FWHM (at 5.9 keV, -25 °C, 2 μs shaping time), and count rate capability of several MHz per cm^2. These detectors also provide one-dimensional spatial resolution on the order of 100 - 300 μm, as a natural consequence of their geometry, which could be useful in some spectroscopy and one-dimensional diffraction applications. In parallel with the detector development, we have been developing the multi-channel low noise integrated circuit pulse-processing electronics for use with the multi-element detectors [2-4].

This paper presents a study of the performance characteristics of highly segmented, high resistivity silicon detectors in response to x-rays in the range 6-25 keV. Our earlier work using the multi-channel silicon strip detectors in x-ray detection revealed that there were some spectral anomalies in the x-ray spectra produced by these detectors [3]. Anomalous peaks appearing at energies below the main photopeak, enhanced spectral background and variations in spectral response, depending on the side of the detector through which the photons were absorbed, were observed. This work reports on the design, simulation, fabrication and testing of silicon strip detectors in an effort to understand and eliminate the spectral anomalies for improved x-ray response.

II. DETECTOR DESIGN AND SIMULATION

Cross-section and top view schematics of a typical one-dimensional silicon strip detector used in this work are shown in Figure 1. The detectors were all fabricated on high resistivity silicon (>5000 ohm-cm) of (100) orientation. The electrode strips were delineated by p^+ boron-implanted strips (2×10^{15} cm^{-2} at 30 keV), separated by oxide, with a planar n^+ contact on the backside of the detector formed using phosphorus-doped polysilicon, which also acts as a gettering layer [5]. Some of the detectors investigated included an aluminum strip on top of the oxide in between the p^+ electrode strips. Several detector designs, which varied in the dimensions of the implanted electrode strips and the interelectrode metal strips, were considered and simulated.

[1] This work is supported by the Director, Office of Energy Research, Biological and Environmental Research, of the U.S. Department of Energy under Contract No. DE-AC03-76SF00098.

The more promising designs were then fabricated and tested. All of the designs were confined by the low noise requirements of the detector: The capacitance of each detector element must be < 0.3 pF and the dark current at room temperature must be <20 pA per element (<1 nA/cm^2) at an operating bias voltage of ~100V. A careful balance between the width and pitch of the electrode strips had to be made, since the interstrip capacitance typically dominates over the back plane capacitance for the dimensions used here [6]. Table 1 shows the dimensions and capacitances of the electrode strips on four of the detectors that are used for examples in this paper. The overall detector area was in the range of 0.5 cm^2.

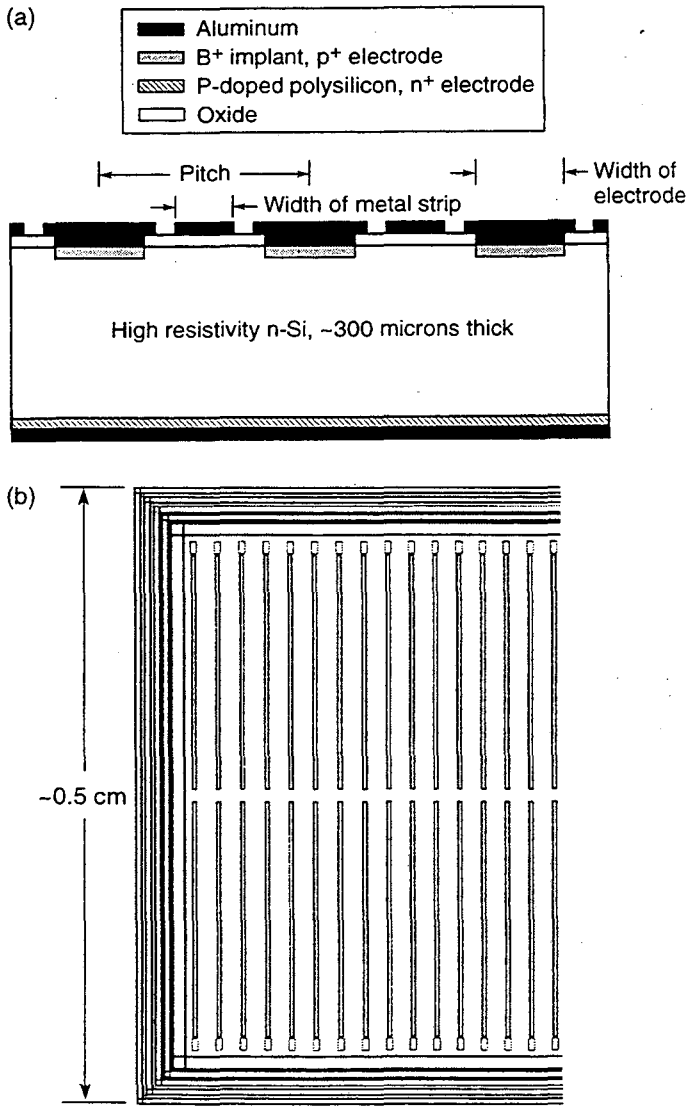

Figure 1. Schematics of detectors, (a) cross-section and (b) top view of layout.

Table 1. Dimensions and capacitances of the electrode strips for the detectors fabricated and tested.

p+ electrode width (μm)	electrode pitch (μm)	strip length (μm)	interelectrode metal strip width (μm)	capacitance (pF)
16	100	2000	--	0.20
16	100	2000	40 (floating)	0.22
16	100	2000	40 (grounded)	0.29
250	300	750	--	0.20

A commercially available software package[2] for semiconductor device simulation was used to model the processing of the detectors as well as the biased devices. This software, similar to others reported in the literature that have been used to model silicon radiation detectors, is based on the PISCES program developed by Stanford University [7], which solves Poisson's equation and the continuity equations for electrons and holes on node points of a finite grid structure superimposed on the device structure. For an explanation of the mathematical and physical models upon which the device simulation software is based, see, for example, references [8-10]. The physical models we used included: Boltzmann statistics, Neumann boundary conditions, Auger recombination, Shockley-Reed-Hall recombination with field and concentration dependent mobility. The material parameters were: n-type silicon doping density of 5 x 10^{11} cm^{-3}, oxide/silicon interface fixed positive charge [11] of 2 x 10^{11} cm^{-2}, boron implant 2 x 10^{15} cm^{-2} at 30 keV, and phosphorus doping of the polysilicon n$^+$ contact of 1 x 10^{19} cm^{-3}.

Figures 2-5 show the calculated potential as a function of depth in the device at 100 V reverse bias, for four detectors. Figure 2 shows the calculated potential in a detector with 16 μm wide implanted electrode strips, on a 100 μm pitch, with 84 μm of oxide separating the electrode strips. The potential drops rather uniformly from the n$^+$ backside contact to the p$^+$ electrodes, but remains high in regions between the p$^+$ electrode strips where there is oxide on the silicon surface. This is due to an electron accumulation layer beneath the oxide/silicon interface, which forms to balance the fixed positive charge of 2 x 10^{11} cm^{-2} at the oxide/silicon interface. Figure 3 shows the potential in a similar detector as in Figure 2, except that 40 μm wide metal strips have been added on top of the oxide, in between the implanted electrode strips. The metal strips are left to float. The addition of the metal strips has caused the potential in between the p$^+$ electrode strips to decrease by a factor of two. Figure 4 shows the calculated potential in the same device as shown in Figure 3, with the metal strips grounded.

[2] Tsuprem4™ and Medici™, from Technology Modeling Associates, Santa Clara, CA. Mention of a particular product does not imply endorsement at the exclusion of others.

Grounding the metal strips results in a further reduction in the potential between the electrode strips, but also results in a 30% increase in capacitance. Figure 5 shows the calculated potential for the detector with the 250 μm wide p^+ electrode strips, on a 300 μm pitch with 50 μm of oxide in between the electrode strips. The reduced amount of oxide compared to the detector shown in Figure 2 has reduced the potential in between the electrode strips from ~45 V to ~15 V. Figure 6 shows the calculated electron concentration as a function of depth beneath the oxide/silicon interface surface, equidistant between the implanted electrode strips, for the configurations shown in Figures 2, 3 and 5. The effects of the potential distribution and electron concentration on the detector performance are discussed in the following section.

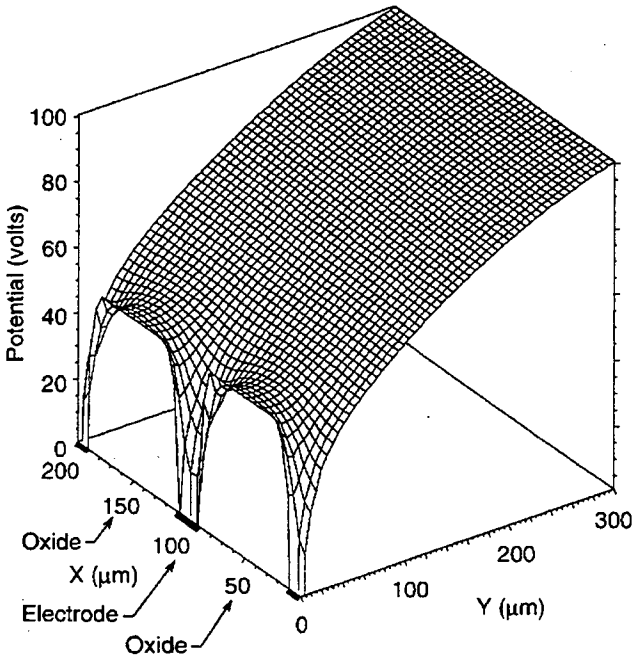

Figure 2. Calculated potential in the detector with 16 μm wide p^+ electrode strips, on a 100 μm pitch, with 100 V bias on the n^+ backside.

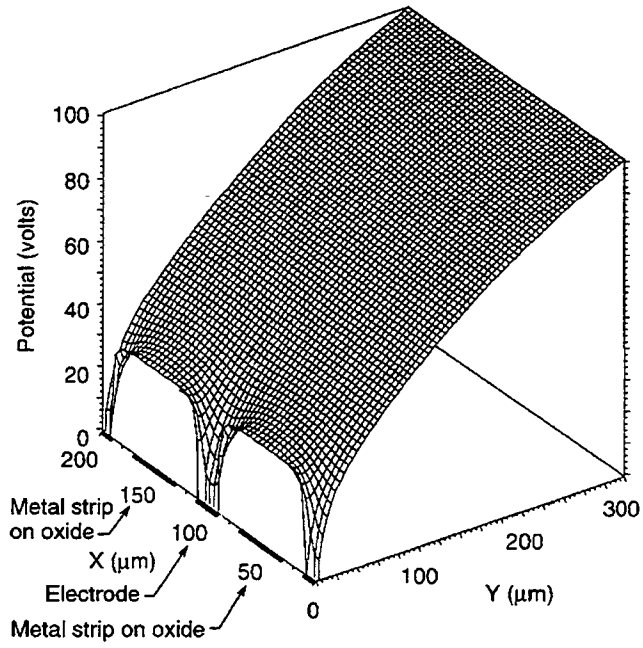

Figure 3. Calculated potential in the detector with 16 μm wide p^+ electrode strips, on a 100 μm pitch, with 40 μm wide metal strips on the oxide in between the p^+ electrode strips, with 100 V bias on the n^+ backside. Metal strips are left to float.

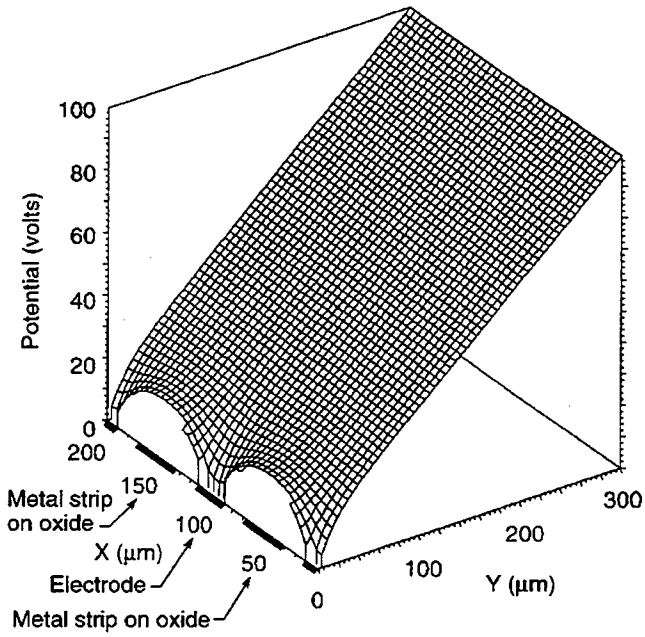

Figure 4. Calculated potential for the same detector as shown in Figure 3, but the metal strips are grounded.

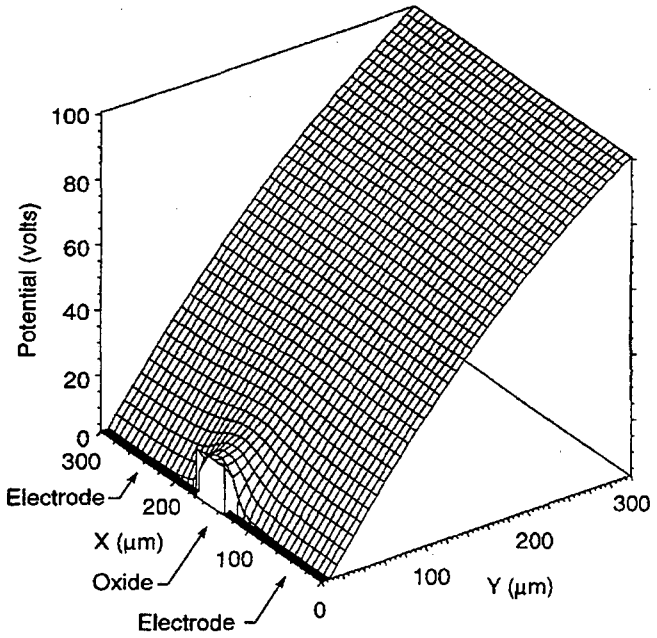

Figure 5. Calculated potential in the detector with 250 μm wide p^+ electrode strips, on a 300 μm pitch, with 100 V bias on the n^+ backside.

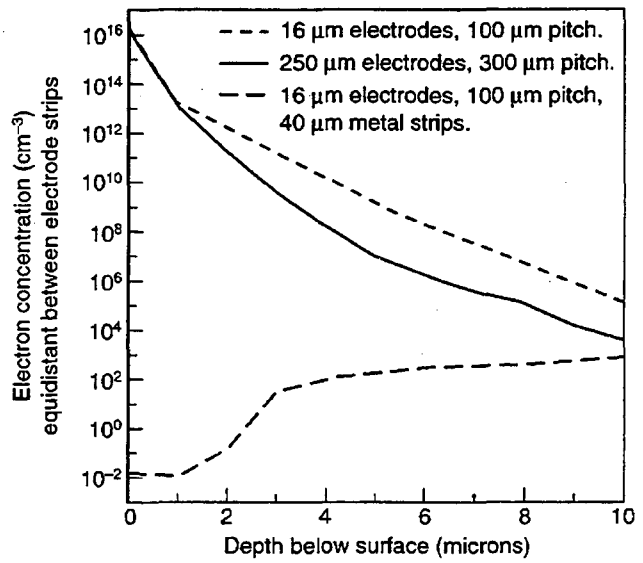

Figure 6. Calculated electron concentration, as a function of depth below stripside surface, for the three detectors of Figures 2, 3 and 5. The plotted electron concentration is taken at a point equidistant between the p^+ electrode strips, which in the case of Figures 2 and 5 is underneath the oxide, and in the case of Figure 3 is underneath the metal strip.

III. X-RAY RESPONSE MEASUREMENTS

The detectors were characterized using ^{55}Fe and ^{109}Cd radioisotope sources, and a 5 μm diameter 8.5 keV synchrotron microprobe beam. The microprobe beam was used to map the detector response as a function of position on the strip side of the detector. Figure 7(a) shows the x-ray response of a detector with 16 μm wide p^+ electrode strips, on a 100 μm pitch, with the microprobe beam impinging directly on the electrode strip. Figure 7(b) shows the response for the same detector when the microprobe beam was directly in between the electrode strips. It is clear that the enhanced background and anomalous peak (this is *not* the silicon escape peak) seen in Figure 7(b) are due to an effect occurring in between the electrode strips. The computer simulations (Figure 2) show that the potential in between the strips just below the oxide/silicon interface, is relatively high and the gradient is relatively flat, and there is also a high electron concentration below the surface (Figure 6). Since the absorption length of 8.5 keV photons in silicon is 60 μm, the detector x-ray response is sensitive to the device characteristics near the surface. Charge carriers are shared among adjacent electrodes and are also trapped in the regions in between the electrode strips, leading to reduced energy events which contribute to the anomalous peaks and spectral background in the x-ray spectra.

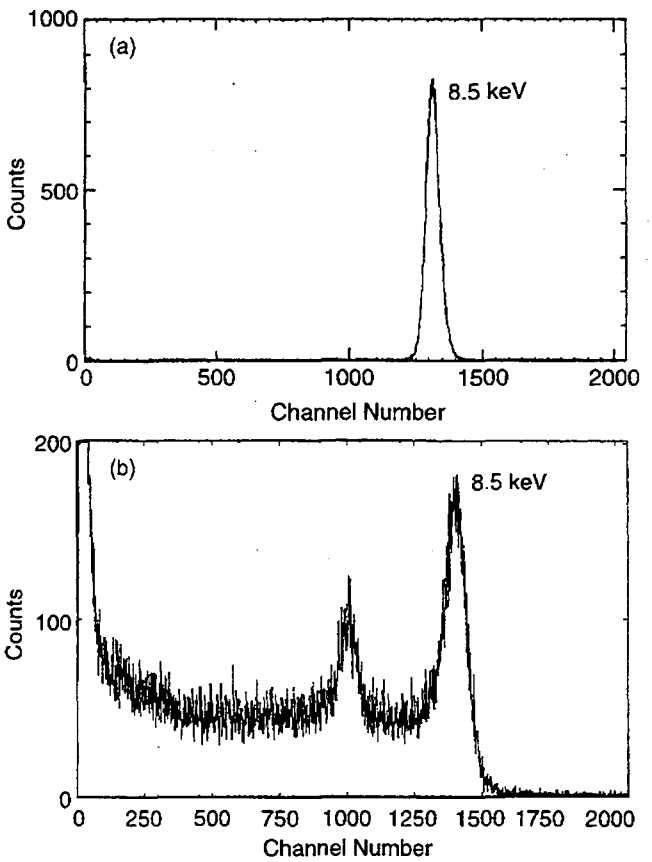

Figure 7. Spectral response to a 5 μm diameter 8.5 keV beam, using the detector with 16 μm wide p^+ electrode strips on a 100 μm pitch, (a) beam directly over the p^+ electrode strip, (b) beam directly in between the p^+ electrode strips.

Figures 8 through 10 show ^{55}Fe x-ray spectra for the three detectors correlating with the simulations of Figures 2, 3 and 5. For all three Figures 8-10, the ^{55}Fe source illuminated the entire detector surface, with absorption through the strip side, with no collimation used. Figure 8 shows a spectrum taken with the detector with the 16 μm wide p^+ electrode strips, on a 100 μm pitch. Although the energy resolution is very good (~264 eV FWHM at 25 °C, and ~200 eV FWHM at -25 °C, at 5.9 keV, 2 μs shaping time), large artificial peaks are again present below the 5.9 and 6.5 keV peaks. The intensity of the anomalous peaks decreases by roughly a factor of two, with the application of the 40 μm wide metal strips on top of the oxide in between the p^+ electrode strips, as is shown in Figure 9. The two-fold decrease in the anomalous peak height corresponds to the two-fold decrease in exposed oxide area. For the data of Figure 9, the metal strips are left to float. The electron accumulation layer is severely reduced in the areas beneath the metal strips, resulting in reduced charge trapping and slightly improved x-ray response. If the metal strips are grounded, the x-ray response does not change appreciably from the case in which the strips are left to float, but the capacitance does increase which is undesirable.

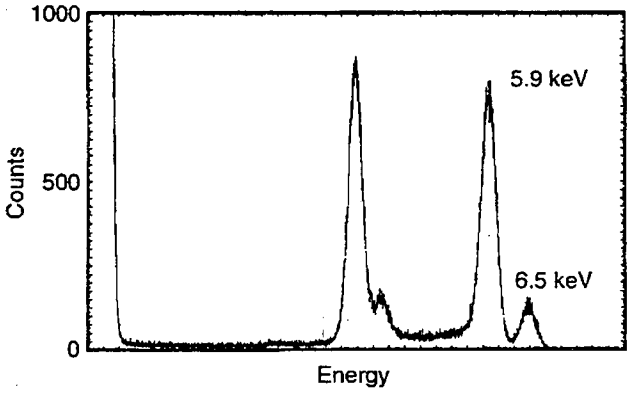

Figure 8. X-ray response to ^{55}Fe for a detector with 16 μm wide p^+ electrode strips, on a 100 μm pitch, photon absorption through stripside (264 eV FWHM @ 5.9 keV, 25 °C, 90V bias, 2 μs shaping time).

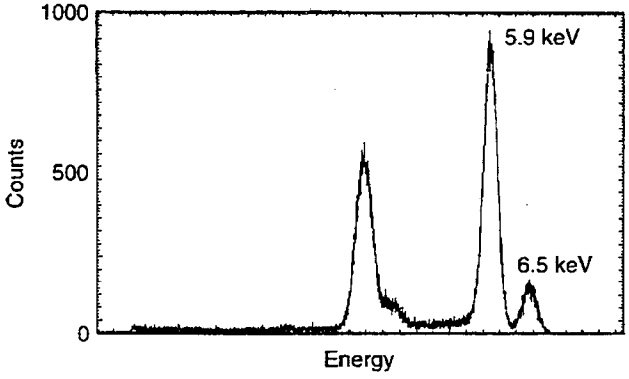

Figure 9. X-ray response to ^{55}Fe for a detector with 16 μm wide p+ electrode strips, on a 100 μm pitch, 40 micron wide metal strips in between the p^+ electrode strips, photon absorption through stripside (231 eV FWHM @ 5.9 keV, 25 °C, 100V bias, 2 μs shaping time).

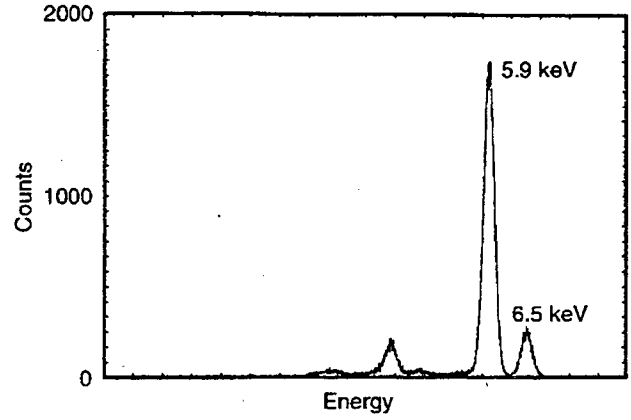

Figure 10. X-ray response to ^{55}Fe for a detector with 250 μm wide p^+ electrode strips, on a 300 μm pitch, photon absorption through stripside (216 eV FWHM @ 5.9 keV, 0 °C, 150V bias, 2 μs shaping time).

Figure 10 shows an eight-fold reduction in the anomalous peak intensity, for the detector with the 250 μm wide p^+ electrodes on a 300 μm pitch, compared to the detector of Figure 8. The ratio of oxide/electrode area has decreased significantly, and the electron concentration below the oxide/silicon interface is less, compared to the detectors of Figure 8, both of which result in improved spectral response.

It is interesting to note that the anomalous peaks in all three of the detectors of Figures 8-10 completely disappear when the detector surfaces are unprotected and are tested under bias in a humid atmosphere. The humidity enables negative charges to migrate to the surface of the detector, which partially balances the fixed positive charge at the oxide/silicon interface [12], and reduces the electron accumulation layer in the silicon. Although elimination of the anomalous peak is desirable, achieving this by operating the detectors in a humid environment leads to increased surface currents and unreliable performance, as has been observed by other researchers [13]. To provide reproducible detector performance, in both dry and humid environments, our detectors are routinely passivated with a polyimide material[3] which provides protection against deleterious environmental effects, maintains the low surface leakage current and does not add to the capacitance of the device.

The detectors were also characterized by illumination through the back side of the detector through the n^+ planar contact. Figure 11 shows the spectrum for ^{55}Fe, back side illumination, for the same detector as is shown in Figure 8 with strip side illumination. It is obvious that the anomalous peaks are absent, although the spectral background is higher

[3] Detectors were passivated with "Ultradel 1414" polyimide from Amoco Chemical. Mention of a particular product does not imply endorsement at the exclusion of others.

than with strip side illumination, and is ~ten times higher than is typically seen in good quality Si(Li) and HPGe detectors. The intensity of the background is a strong function of bias, and decreases by a factor of two between 80 V and 150 V. Unfortunately, the detectors typically broke down at operating voltages >200 V, and so we were not able to determine to what extent further increases in bias voltage would result in further decreases in spectral background. Including improved guard ring structures [14],[15] on future detectors may provide the opportunity to operate the detectors at higher voltages.

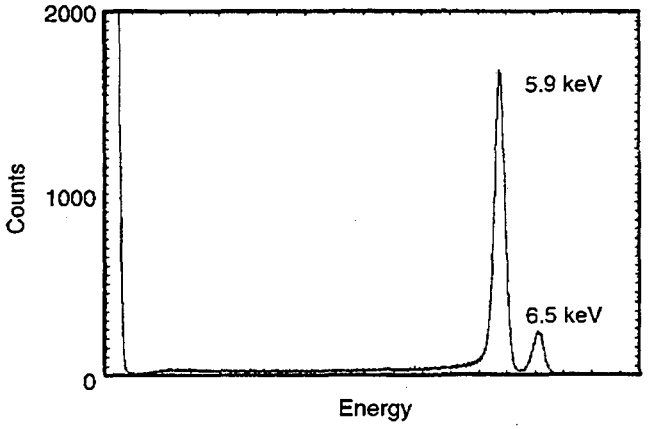

Figure 11. X-ray response to ^{55}Fe for a detector with 16 μm wide p^+ electrode strips, on a 100 μm pitch, photon absorption through the n^+ backside (215 eV FWHM @ 5.9 keV, -25 °C, 250V bias, 2 μs shaping time).

As mentioned earlier, there are two main sources of spectral background in these detectors: reduced energy events due to charge *loss* and charge *sharing*. Charge *loss* is defined as charge lost from the carriers generated from the absorption of a photon, which then does not contribute to the induced signal on an electrode. On the other hand, charge *sharing* is defined as the splitting of charge onto two (or more) neighboring electrodes, which results in a reduced signal on each of the electrodes. Coincidence measurements, using 5.9 keV photons absorbed through the back side of a 100 μm pitch detector, show that ~16% of the total events are shared with the two neighboring strips, which is expected based on the pitch and charge cloud diameter. The 5.9 keV photons are absorbed close to the detector surface, and for the case of backside illumination, the charge carriers must drift through most of the 300 μm thickness before reaching the signal electrodes. During the time it takes to drift 300 μm, the charge cloud increases to approximately 10 μm in diameter. For the detectors with a 300 μm pitch, the shared events decrease to ~6%. Since the total number of counts in the background is a strong function of bias, the percentage of the events in the background due to charge sharing is also a function of bias. For example, in Figure 11 (taken at 250 V bias), charge sharing accounts for ~60% of the total counts in the background below the 5.9 keV peak.

IV. Discussion

In summary, the detectors with the 250 μm wide p^+ electrodes, on a 300 μm pitch, offered the best performance of the designs discussed here (see Figure 11). The wide pitch minimized charge sharing among neighboring strips, which minimized the spectral background. The larger electrode/oxide ratio maximized the detector area with good charge collection and minimized the detector area with charge trapping. Illumination through the backside of the detector resulted in clean x-ray spectra, with no spurious peaks, although the charge sharing increased compared with stripside illumination for the low energy photons which are absorbed close to the detector surface. For higher energy photons, which are absorbed throughout the detector volume, either backside or stripside illumination was adequate (see Figure 12, ^{109}Cd spectrum). The use of such wide strips resulted in a relatively large capacitance per unit length of strip, and thus the strips needed to be kept quite short (~750 μm) for the low capacitances targeted here. This then reduces the overall detector area that can be covered using the one-dimensional array design.

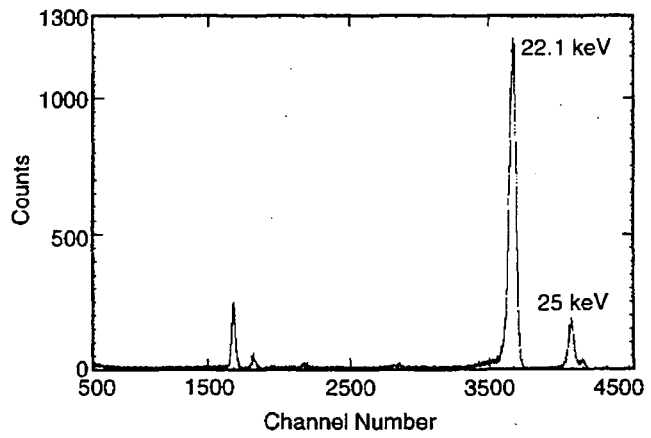

Figure 12. ^{109}Cd spectrum using a detector with 250 μm wide p^+ electrode strips on a 300 μm pitch, photon absorption through the n^+ backside (-25 °C, 2 μs shaping time). X-ray peaks at lower energy are due to fluorescence of the metal collimator used in this measurement.

Other paths were pursued in the detector designs and simulations, but the detectors were not fabricated due to the unacceptable compromises discussed below:

For electrode strip separations of <50 μm, the interstrip capacitance became unacceptably high. Electrode strip separations >85 μm led to large regions in between the strips with charge trapping problems due to the potential distribution and electron accumulation layer. Pitches <100 μm led to increased charge sharing, while pitches >300 μm led to short "strips", actually pixel-like elements, which covered an unacceptably small detector area.

The metal strips on the oxide in between the p^+ electrode strips reduced the electron accumulation layer beneath the oxide/silicon interface, which then reduced the charge

trapping in that region. However, for this approach to improve the spectral response significantly, the metal strip would have to be wide enough to cover a substantial amount of the exposed oxide, which would then decrease the separation between the metal strip and the p^+ electrode and increase the capacitance. Grounding or applying voltage to the metal strips could be used to shape the potential distribution in between the electrode strips, and thereby possibly improve charge collection, but again the capacitance increases undesirably.

V. Conclusions

Our high resistivity silicon detectors with the best measured x-ray performance to date have 250 μm wide p^+ electrodes, on a 300 μm pitch, with photon absorption through the n^+ backside. The energy resolution, with the LBNL multi-channel integrated circuit preamplifier is very good (~200 eV FWHM at 5.9 keV, -10 ^{o}C, 2 μs shaping time); the charge sharing, and thus the spectral background, is minimized using the wide strip pitch, and there are no spurious peaks in the x-ray spectra.

VI. Acknowledgments

We would like to thank Nicole Milas for assistance with the computer modeling and George Zizka for the detector wire-bonding. We would also like to thank Nicholas Palaio and Steve Holland for invaluable consultations and assistance with the detector fabrication.

VII. References

[1] D.C. Koninsberger and R. Prins, eds., X-Ray Absorption: Principles, Applications, Techniques of EXAFS, SEXAFS and XANES, New York: John Wiley and Sons, 1988.

[2] B. Ludewigt, J. Jaklevic, I. Kipnis, C. Rossington and H. Spieler, "A high rate, low noise x-ray silicon strip detector system", *IEEE Trans. Nucl. Sci*, vol. 41 (4), pp.1037-1041, 1994.

[3] B. Ludewigt, C. Rossington, I. Kipnis and B. Krieger, "Progress in multi-element silicon strip detectors for synchrotron XRF applications", *IEEE Trans. Nucl. Sci.*, vol. 43, pp.1442-1445, 1996.

[4] B. Kreiger, I. Kipnis and B. Ludewigt, "XPS: A multi-channel preamplifier-shaper IC for x-ray spectroscopy", presented at the IEEE Nuclear Science Symposium, Albuquerque, NM, Nov. 9-15, 1997.

[5] S. Holland, "Fabrication of detectors and transistors on high resistivity silicon", *Nucl. Instr. Meth.*, A275, pp.537-541, 1989.

[6] E. Barberis, N. Cartiglia, D. Hutchinson, J. Leslie, C. Le Vier, J. Rahn, W. Rowe, H.F.-W. Sadrozinski, K. Yamamoto, K. Yamamura, T. Ohsugi, Y. Unno, T. Aso, H. Miyata and N. Tamura, "Measurement of interstrip and coupling capacitances of silicon microstrip detectors", *University of Santa Cruz publication no. SCIPP 92/14*, Conference Proceedings of the 1992 IEEE Nuclear Science and Medical Imaging Symposium, Orlando, FL.

[7] M.R. Pinto, S.R. Conor and R.W. Dutton, "PISCES2: Poisson and continuity equation solver", *Stanford Electronics Laboratory Technical Report*, Stanford University, Palo Alto, CA, 1984.

[8] E.M. Buturla, P.E. Cottrell, B. M. Grossman and K.A. Salsburg, "Finite-element analysis of semiconductor devices: The Fielday program", *IBM J. Res. Develop.*, vol. 25 (4), pp.218-231, July 1981.

[9] S.E. Laux and R.G. Byrnes, "Semiconductor device simulation using generalized mobility models", *IBM J. Res. Develop.*, vol. 29 (3), pp.289-301, May 1985.

[10] M. Berger and E. Stein, "Two-dimensional simulation of integrated detectors and electron devices", *Nucl. Instr. Meth.*, A253, pp.382-385, 1987.

[11] S.M. Sze, Physics of Semiconductor Devices, 2nd edition, p.379, New York: John Wiley and Sons, 1981.

[12] W. Shockley, W.W. Hooper, H.J. Queisser and W. Shroen, "Mobile electric charges on insulating oxides with application to oxide covered silicon p-n junctions", *Surface Science*, vol. 2, pp.277-287, 1964.

[13] A. Longoni, M. Sampietro and L. Struder, "Instability of the behavior of high resistivity silicon detectors due to the presence of oxide charges", *Nucl. Instr. Meth.*, A288, pp.35-43, 1990.

[14] L. Evenson, A. Hanneborg, B. Sundby Avset and M. Nese, "Guard ring design for high voltage operation of silicon detectors", *Nucl. Instr. Meth.*, A337, pp.44-52, 1993.

[15] B. Sundby Avset and L. Evenson, "The effect of metal field plates on multiguard ring structures with floating p^+ guard rings", *Nucl. Instr. Meth.*, A377, pp.397-403, 1996.

Ernest Orlando Lawrence Berkeley National Laboratory
One Cyclotron Road | Berkeley, California 94720

Prepared for the U.S. Department of Energy under Contract No. DE-AC03-76SF00098